Available online at www.sciencedirect.com
SCIENCE DIRECT
Applied Radiation and Isotopes 64 (2006) 823–829
Applied Radiation and Isotopes
www.elsevier.com/locate/apradiso

Detection of spallation neutrons and protons using the ^{nat}Cd activation technique in transmutation experiments at Dubna

M. Manolopoulou[a,*], S. Stoulos[a], M. Fragopoulou[a], R. Brandt[b], W. Westmeier[b], M. Krivopustov[c], A. Sosnin[c], M. Zamani[a]

[a]*Physics Department, Aristotle University of Thessaloniki, Thessaloniki 54124, Hellas,Greece*
[b]*Philipps Universität, D-35032 Marburg, Germany*
[c]*Joint Institute for Nuclear Research, 141980 Dubna, Russia*

Received 28 November 2005; received in revised form 8 January 2006; accepted 27 January 2006

Abstract

Various spallation sources have been used to transmute long-lived radioactive waste, mostly making use of the wide energy neutron fluence. In addition to neutrons, a large number of protons and gamma rays are also emitted from these sources. In this paper ^{nat}Cd is proved to be a useful activation detector for determining both thermal–epithermal neutron as well as secondary proton fluences. The fluences measured with ^{nat}Cd compared with other experimental data and calculations of DCM-DEM code were found to be in reasonable agreement. An accumulation of therma–epithermal neutrons around the center of the target (i.e. after approx. 10 cm) and of secondary protons towards the end of the target is observed.

Keywords: Spallation neutron and proton detection; ^{nat}Cd; Activation analysis

1. Introduction

Intense neutron fluences can be produced via spallation reactions in a solid target (e.g. protons on a Pb or Pb(U) target). Such sub-critical accelerator driven system (ADS) can be used for transmutation of long-lived radioactive waste by neutron capture or neutron induced fission (Carminati et al., 1993; Andriamonje et al., 1995; Krivopustov et al., 1997; Wan et al., 1998). The effectiveness of an ADS depends highly on the fluence and energy distribution of secondary particles. Various threshold activation detectors, such as Au, La, U, In, W. etc., have been applied in several experimental set-ups (Brandt et al., 1999; TARC, 1999; Wan et al., 2001; Krivopustov et al., 2003) in order to determine the neutron fluence in specific energy ranges.

During the spallation process, accompanying the neutrons, intense fields of secondary charged hadrons (mainly protons) and a large amount of gamma rays are also emitted from the target. In order to cope with the high radiation levels of a spallation environment (e.g. for dosimetric purposes), the secondary hadrons and gamma rays have to be determined, too. Although secondary neutron production around spallation targets has been thoroughly studied (Brandt et al., 1999; TARC, 1999; Wan et al., 2001; Krivopustov et al., 2003), there are quite limited data available for other hadrons and gamma rays, as well (Kovalenko et al., 1994; Bauer, 2001). Especially, the secondary proton fluence determination is of high interest, regarding not only radiolytic effects but also the possibility of additional transmutation channels by proton induced reactions.

Therefore an activation detector, which has response to both spallation neutrons as well as secondary protons, would be a useful tool. ^{nat}Cd is a good candidate because of its high cross section for neutron capture in

*Corresponding author. Tel.: +30 231 099 8217; fax: +30 231 099 8217.
E-mail address: metaxia@auth.gr (M. Manolopoulou).

0969-8043/$ - see front matter © 2006 Elsevier Ltd. All rights reserved.
doi:10.1016/j.apradiso.2006.01.014

the thermal-epithermal region. Additionally, it has considerable cross section for (p,xn) reactions in the proton energy range from 10 up to100 MeV (Nortier et al., 1990; Zaitseva et al., 1990; Tárkányi et al., 1994), which matches to the energy range of secondary protons produced at spallation targets (Kovalenko et al., 1994; Bauer, 2001). In this paper experiments investigating the thermal–epithermal neutron fluence, determined via the $^{nat}Cd(n,x)^{115}Cd$ routes and the secondary proton fluence determined via the $^{nat}Cd(p,x)^{111}In$ processes are presented. These experiments were accomplished on the GAMMA-2 experimental transmutation set-up in Dubna.

2. Experimental

The GAMMA-2 transmutation set-up, where the spallation target is a lead cylinder of 8 cm diameter and 20 cm length covered by a paraffin moderator of 6 cm thickness, is sketched in Fig. 1. The Pb target was irradiated with a 1 GeV proton beam with total fluence of $(7.6\pm0.3)\times10^{12}$ protons at the Laboratory of High Energies, JINR, Dubna, Russia. Two general types of measurements were performed on the GAMMA-2 set-up:

(A) Neutron fluence measurements with ^{nat}Cd detectors and several supplementary techniques such as solid state nuclear track detectors (used as particle and fission fragment detectors e.g. CR39 covered with boron and Makrofol covered with ^{235}U, ^{238}U, ^{232}Th) as well as threshold activation detectors (e.g. La, Au, Bi) for monitoring the neutron spectrum emitted (Brandt et al., 1999; Krivopustov et al., 2003).
(B) Transmutation rate measurements for several long-lived radioactive waste nuclides ^{129}I, ^{237}Np and others through (n,γ) reactions (Wan et al., 2001; Adam et al., 2002)

In this experiment five samples of natural Cd (mass approx. 2 g, purity 99.9%) were irradiated on top of the Pb/Paraffin target (Fig. 1). Starting one day after the end of irradiation, the samples were measured several times during 2 weeks using a low-level HPGe γ-ray spectrometry system. The system consists of a coaxial detector with 42% efficiency, 2.2 keV resolution for 1.33 MeV photons (^{60}Co) and shielded by 4″ low-background Pb with an inner lining of 1 mm Cd and 1 mm Cu, a high voltage power supply, an amplifier with pile-up rejector and a computer based multichannel analyzer.

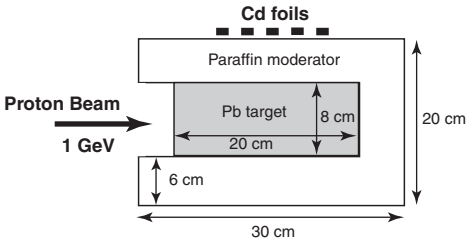

Fig. 1. The GAMMA2 (Pb/Paraffin target) set-up.

3. Results and discussion

In the γ-spectra measured in multichannel-scaling mode from the activated Cd foils several isotopes were quantified. Most isotopes can be produced by different n- or p-induced reactions. Table 1 lists those reactions which have cross-section exceeding 10 mb. Two isotopes were of particular interest:

(a) ^{111}In emitting 171 and 245 keV γ-rays with a decay constant of $2.86\times10^{-6}\,s^{-1}$ and
(b) ^{115}Cd emitting 261, 336, 492 and 528 keV γ-rays with a decay constant of $3.60\times10^{-6}\,s^{-1}$. The 336 keV γ-ray is emitted by ^{115m}In which is decay product of ^{115}Cd. At the time of measurement ^{115m}In was in secular equilibrium with its parent due to its large decay constant of $4.29\times10^{-5}\,s^{-1}$.

The quantification of ^{115}Cd was made over the decay curves of the two most intense γ-rays: 336 keV ($I_\gamma=45.9\%$) and 528 keV ($I_\gamma=27.4\%$) for which decay constants of $(3.55\pm0.05)\times10^{-6}\,s^{-1}$ and $(3.65\pm0.06)\times10^{-6}\,s^{-1}$ were fitted, respectively (see Fig. 2). Likewise, analyzing the decay curves of ^{111}In γ-rays 171 keV ($I_\gamma=90.7\%$) and 245 keV ($I_\gamma=94.1\%$), decay constants of $(2.76\pm0.04)\times10^{-6}$ and $(2.85\pm0.04)\times10^{-6}\,s^{-1}$ were fitted, respectively (see Fig. 3).

The isotope ^{115}Cd can be produced from the ^{nat}Cd foil due to the following reactions:

$$\begin{matrix}{}^{114}\mathrm{Cd}\,(n,\gamma)\\ \{28.73\%\}\end{matrix}\qquad\qquad \begin{matrix}\beta^-,E_\gamma=528\ \mathrm{keV}\\ \longrightarrow\end{matrix}$$

$$\begin{matrix}{}^{116}\mathrm{Cd}(n,2n)\\ \{7.49\%\}\end{matrix}\quad\rightarrow\quad {}^{115}\mathrm{Cd}\quad [T_{1/2}=2.228\mathrm{d}]$$

$$\begin{matrix}{}^{115m}\mathrm{In}.\\ [T_{1/2}=4.486\ \mathrm{h}]\end{matrix}\qquad\qquad \begin{matrix}IT(95\%),E_\gamma=336\ \mathrm{keV}\\ \longrightarrow\\ \beta^-(5\%)\\ \longrightarrow\end{matrix}\qquad \begin{matrix}{}^{115}\mathrm{In}\\ \\ {}^{115}\mathrm{Sn}\end{matrix} \tag{1}$$

Table 1
Isotopes identified in the γ-spectra of the activated Cd foils

Produced isotope	Reaction
^{115}Cd	$^{114}Cd(n,\gamma)$ and $^{116}Cd(n,2n)$
^{111}In	$^{nat}Cd(p,x)^{111}In$
^{105}Ag	$^{106}Cd(n,2n)^{105}Cd\rightarrow{}^{105g}Ag$ and $^{106}Cd(n,np)$
^{106m}Ag	$^{106}Cd(n,p)$
^{110m}Ag	$^{110}Cd(n,p)$ and $^{111}Cd(n,np)$
^{111}Ag	$^{111}Cd(n,p)$ and $^{112}Cd(n,np)$

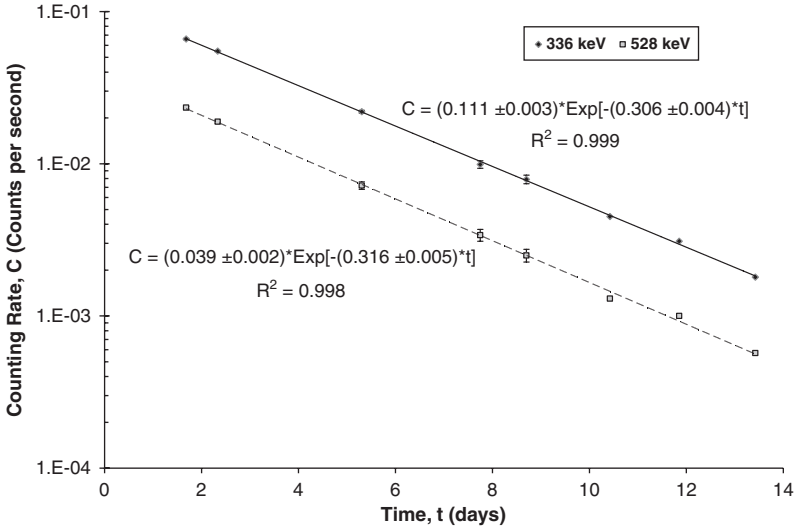

Fig. 2. Decay curve of 336 and 528 keV γ-rays emitted by ^{115}Cd.

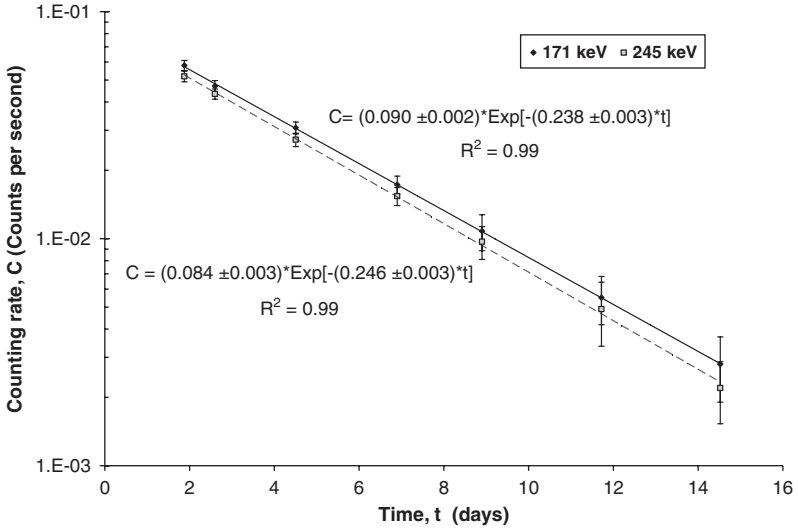

Fig. 3. Decay curve of 171 and 246 keV γ-rays emitted by ^{111}In.

while the ^{111}In isotope could originate due to the following ones:

$$\left.\begin{array}{l} {}^{110}_{\{12.49\%\}}\mathrm{Cd}\,(p,\gamma) \\ {}^{111}_{\{12.80\%\}}\mathrm{Cd}\,(p,n) \\ {}^{112}_{\{24.13\%\}}\mathrm{Cd}\,(p,2n) \\ {}^{113}_{\{12.22\%\}}\mathrm{Cd}\,(p,3n) \\ {}^{114}_{\{28.73\%\}}\mathrm{Cd}\,(p,4n) \\ {}^{116}_{\{7.49\%\}}\mathrm{Cd}\,(p,6n) \end{array}\right\} \rightarrow {}^{111}_{[T_{1/2}=2.805\mathrm{d}]}\mathrm{In} \xrightarrow{\varepsilon,E_\gamma=245{,}171\ \mathrm{keV}} {}^{111}\mathrm{Cd} \qquad (2)$$

Numbers in swift brackets denote the natural abundance of that isotope.

Considering that the same produced isotope can originate from several Cd isotopes by different reaction channels, the definition of an effective cross section is recommended in order to determine the neutron and secondary proton fluences. The following case study was done:

3.1. Neutron induced reaction

The total production rate of ^{115}Cd nuclei ($N_{^{115}\mathrm{Cd}}$) during an irradiation is given as

$$\frac{\mathrm{d}N_{^{115}\mathrm{Cd}}}{\mathrm{d}t} = f_{^{114}\mathrm{Cd}} N_{^{\mathrm{nat}}\mathrm{Cd}} \int \sigma_{^{114}\mathrm{Cd}(n,\gamma)}(E)\Phi_n(E)\,\mathrm{d}E$$

(^{114}Cd(n,g) reaction rate, R_c)

$$+ f_{^{116}\mathrm{Cd}} N_{^{\mathrm{nat}}\mathrm{Cd}} \int \sigma_{^{116}\mathrm{Cd}(n,2n)}(E)\Phi_n(E)\,\mathrm{d}E$$

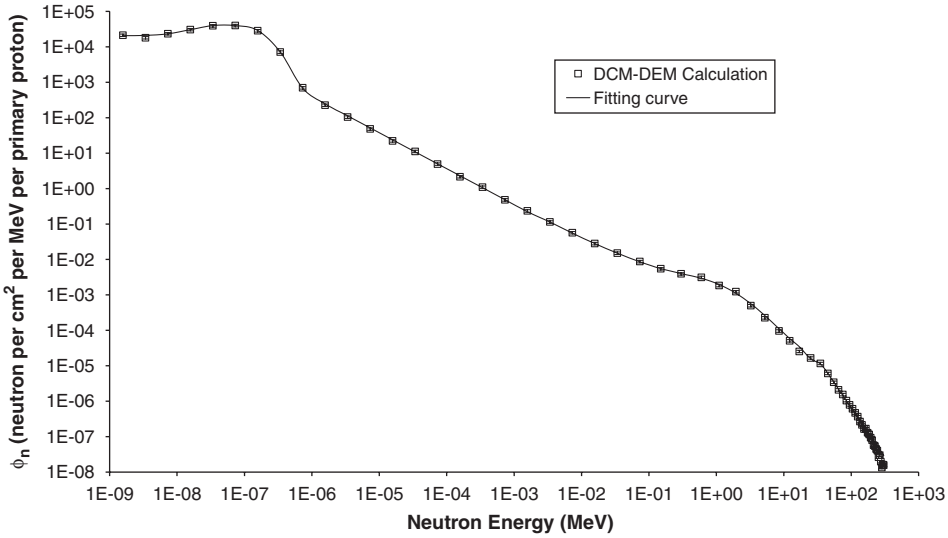

Fig. 4. The energy dependent neutron fluence obtained using the Dubna Cascade Model (DCM-DEM) on the top of GAMMA2 set-up irradiated by a proton beam of 1 GeV.

$$(^{116}\mathrm{Cd}(n,2n)\ \text{reaction rate},\ R_\mathrm{f}) - \lambda N_{^{115}\mathrm{Cd}} \quad (^{115}\mathrm{Cd}\ \text{decay}), \tag{3}$$

where $\sigma_{^{114}\mathrm{Cd}(n,\gamma)}(E)$ and $\sigma_{^{116}\mathrm{Cd}(n,2n)}(E)$ is the reaction cross sections in cm^2, $\Phi_n(E)$ is the neutron flux in [$n\,\mathrm{cm}^{-2}\,\mathrm{s}^{-1}\,\mathrm{MeV}^{-1}$], f is the natural abundance of each Cd isotope (28.73% for ^{114}Cd and 7.49% for ^{116}Cd) and $N_{^{\mathrm{nat}}\mathrm{Cd}}$ is the number of Cd nuclei in the sample. According to the energy dependent cross sections obtained from the ENDF/B-VI (300 K) library, the production of ^{115}Cd via the ^{114}Cd(n,γ) reaction is more efficient in the energy range up to 1 keV due to thermal–epithermal neutrons, while the production of ^{115}Cd via ^{116}Cd$(n,2n)$ reaction is mainly due to fast neutrons in the energy range from 10 to 20 MeV.The actual production rates in units of [nuclei s^{-1}] of the two production channels are the follows:

$$R_\mathrm{c} = 28.73\% N_{^{\mathrm{nat}}\mathrm{Cd}} \int_{0\ \mathrm{MeV}}^{10^{-3}\ \mathrm{MeV}} \Phi_{n\text{-th\_epith}}(E)\sigma_{^{114}\mathrm{Cd}(n,\gamma)}(E)\,\mathrm{d}E, \tag{4}$$

$$R_\mathrm{f} = 7.49\% N_{^{\mathrm{nat}}\mathrm{Cd}} \int_{10\ \mathrm{MeV}}^{20\ \mathrm{MeV}} \Phi_{n\text{-fast}}(E)\sigma_{^{116}\mathrm{Cd}(n,2n)}(E)\,\mathrm{d}E, \tag{5}$$

where Φ_n is the energy depending neutron flux [$n\,\mathrm{cm}^{-2}\,\mathrm{s}^{-1}\,\mathrm{MeV}^{-1}$].

To estimate the contribution of both reaction rates (R_c and R_f), the neutron fluence on top of the Pb/Paraffin target was calculated (Sosnin, 2003) using the high-energy transport code DCM-DEM[1] (see Fig. 4). A fitting procedure was applied to the energy dependent neutron fluence $\Phi_\mathrm{n}(E)$ in order to obtain the necessary function at any specific energy range (Stoulos et al., 2003). Fitting procedures were also applied to the data of the energy dependent cross sections. Gaussian–Lorentzian function was fit to each resonance peak of the (n,γ) reaction and a Chester–Cram peak function was used for the $(n,2n)$ reaction (Stoulos et al., 2003). Thus, using Eqs. (4) and (5), the proportion of the production rates resulted to be $R_\mathrm{c}/R_\mathrm{f} = 17 \pm 3$. This value clearly shows that the production of ^{115}Cd comes mainly from the ^{114}Cd(n,γ) reaction and the determined neutron fluence, using the $^{\mathrm{nat}}$Cd foil for monitoring the emitted neutron spectrum, practically corresponds to the thermal–epithermal region up to 1 keV.

3.2. Proton induced reaction

The total production rate of ^{111}In nuclei during the irradiation is given by an equation similar to Eq. (3), wherein six different production channels are involved. To examine the contribution of each reaction path to ^{111}In nuclei production, the secondary proton fluence on top of the Pb/Paraffin target was estimated using the DCM-DEM code (Sosnin, 2003) and a fitting procedure was applied to obtain the necessary function at any specific energy range (see Fig. 5). The energy spectrum of the proton fluence from the Pb/Paraffin target can be described by an exponential background function superimposed by a log-normal peak extending from 20 up to 100 MeV with a centroid around 50 MeV ($R^2 = 96\%$). The calculated secondary proton spectrum using the DCM-DEM code shows good agreement when compared with the measured one for similar targets irradiated with energy resembling proton beams (Kovalenko et al., 1994; Bauer, 2001).

For the proton energy range 10 MeV $\leqslant E_\mathrm{p} \leqslant$ 100 MeV the experimental cross section data of the $^{\mathrm{nat}}$Cd$(p,x)^{111}$In

[1]The DCM-DEM code is a Dubna version of the cascade-evaporation approach, similar to the Bertini model. This is supplied with high-energy fission and pre-equilibrium evaporation, and the calculations correspond to the moderator surface fluence.

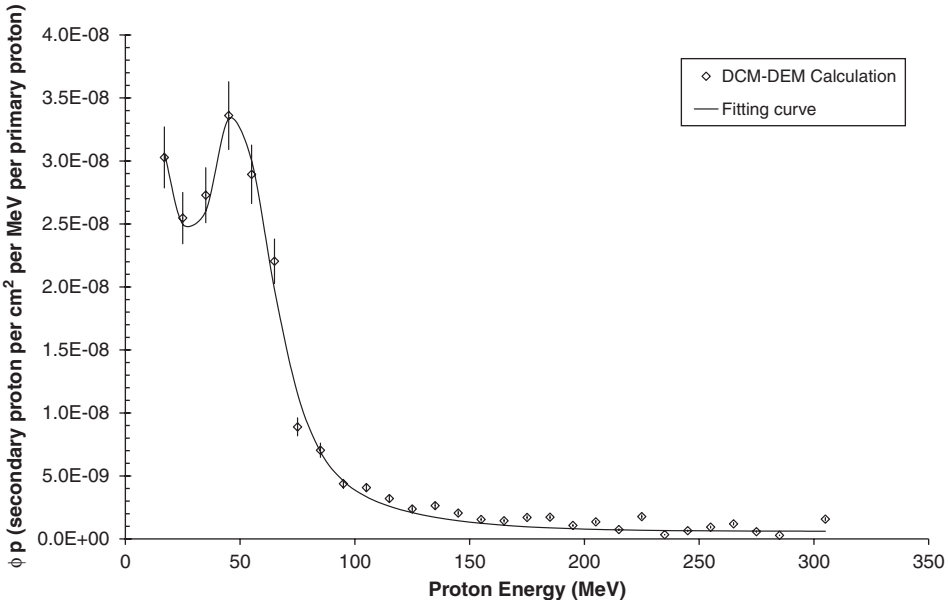

Fig. 5. The energy dependent secondary proton fluence obtained using the Dubna Cascade Model (DCM-DEM) for the top of GAMMA2 setup irradiated by a proton beam of 1 GeV.

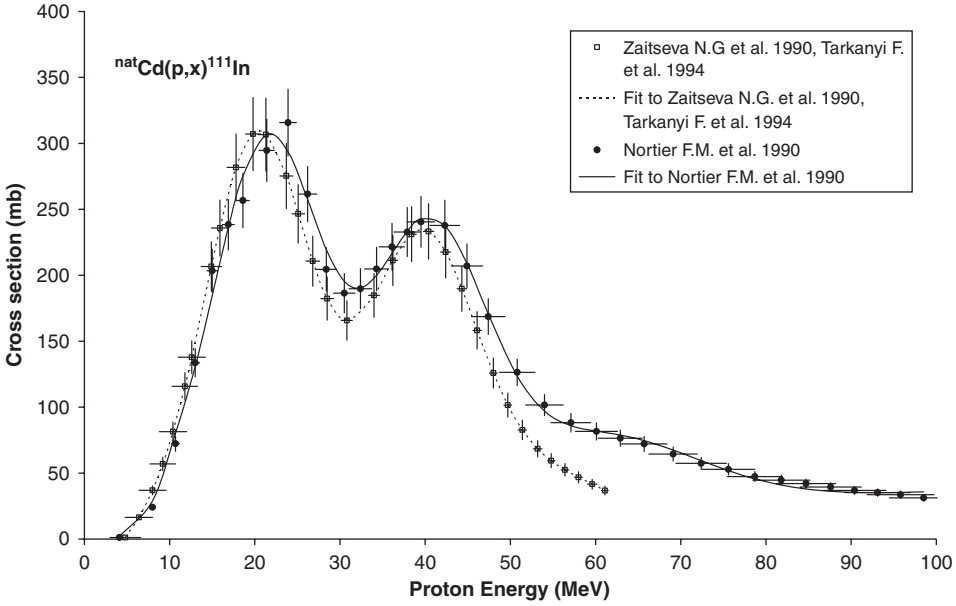

Fig. 6. Literature excitation function data for the ^{nat}Cd $(p,x)^{111}$In reaction.

reaction (Nortier et al., 1990; Zaitseva et al., 1990; Tárkányi et al., 1994) were taken into account and a fitting procedure was applied, yielding a goodness-of-fit variable $R^2 = 0.98$ (see Fig. 6). In both sets of experimental data the ^{nat}Cd$(p,x)^{111}$In cross section fit indicates that Gaussian peaks sit on a quadratic background function. The first Gaussian with a centroid at 22 ± 1 MeV originates mainly from the ^{112}Cd$(p,2n)$ reaction (Tárkányi et al., 1994), whereas the second one with a centroid at 40 ± 1 MeV is a conflation of ^{113}Cd$(p,3n)$ and ^{114}Cd$(p,4n)$ reactions (Zaitseva et al., 1990). At the Nortier et al. (1990) data set a third Gaussian peak appears with a centroid at 60 ± 3 MeV which may originate from the ^{116}Cd$(p,6n)$ reaction.

The total experimental fluence of neutrons and secondary protons F_{exp} (cm^{-2} per primary proton) was estimated using the formula

$$F_{exp} = \frac{N_{produced}}{N_{irradiated} F_p \sigma_{eff}}, \quad (6)$$

where $N_{produced}$ is the total number of produced nuclei, $N_{irradiated}$ is the total number of irradiated Cd nuclei, F_p is the proton beam fluence and σ_{eff} is the effective cross

section of each reaction path. The effective cross section σ_{eff} was estimated as follows:

$$\sigma_{\text{eff}} = \frac{\int_{E_1}^{E_2} \Phi(E)\sigma(E)\,\mathrm{d}E}{\int_{E_1}^{E_2} \Phi(E)\,\mathrm{d}E}, \quad (7)$$

where $\Phi(E)$ is the energy dependent fluence of neutrons or secondary protons spectrum and $\sigma(E)$ is the excitation function of the relevant reaction. The total number of produced nuclei was calculated from the decay curve of selected γ-rays of ^{115}Cd and ^{111}In, see Figs. 2 and 3. For these measurements, performed with the γ-spectroscopy system, an essential summation correction factor has been calculated for the specific sample geometry.

The obtained effective cross sections of the $^{\text{nat}}\text{Cd}(n,x)^{115}\text{Cd}$ and $^{\text{nat}}\text{Cd}(p,x)^{111}\text{In}$ reactions for the energy ranges of secondary neutrons and protons were estimated by Eq. (7) and are presented in Table 2. Using the obtained effective cross sections and Eq. (6), the thermal–epithermal neutron and secondary proton fluences in the energy range from 10 up to 100 MeV along the Pb/Paraffin target were determined and they are presented in Fig. 7. For the $^{\text{nat}}\text{Cd}(p,x)^{111}\text{In}$ reaction, an effective cross section of $0.15 \pm 0.02\,b$ was used taking into account only the experimental data set from Nortier et al. (1990), as the energy region of 10 up to 100 MeV is included only in this data set.

Table 2
The effective cross-sections of nuclear reactions induced by neutrons and protons on $^{\text{nat}}$Cd in the corresponding energy range for GAMMA2 setup irradiated by a proton beam of 1 GeV

Reaction	Energy range	Effective cross section σ_{eff} (b)
$^{\text{nat}}\text{Cd}(n,x)^{115}\text{Cd}$	Up to 1 keV	0.14 ± 0.03
$^{\text{nat}}\text{Cd}(p,x)^{111}\text{In}$	10–100 MeV	0.14 ± 0.02[a]
		0.15 ± 0.02[b]

[a]Using cross section data from Zaitseva et al. (1990) and Tárkányi et al. (1994).
[b]Using cross section data from Nortier et al. (1990).

The value of the thermal–epithermal neutron fluence determined by Cd foils, $3.1 \pm 0.6 \times 10^{-3}$ neutrons/cm^2/primary proton, is comparable to the result from model calculations with the DCM-DEM code, $3.5 \pm 0.5 \times 10^{-3}$ neutrons/cm^2/primary proton, after integration over the corresponding energy range up to 1 keV. The thermal–epithermal neutron fluence distribution along the target shows a maximum around the middle of the Pb target, as it was expected from previous studies using other methods (Adloff et al., 1999; Hashemi-Nezhad et al., 1999).

The values of the secondary proton fluences in the energy range from 10 up to 100 MeV determined by Cd foils are presented in Fig. 7. They are in acceptable agreement with the values measured at similar targets and proton beams of comparable energies (Kovalenko et al., 1994; Bauer, 2001). They also compare reasonable well with the result from model calculations ($5.6 \pm 0.3 \times 10^{-5}$ protons/cm^2/primary proton) using the DCM-DEM code. Regarding the secondary proton fluence distribution along the target, an increase is found towards the end of the Pb target, but due to the limited number of measurements along the target and the statistical uncertainties involved no significant conclusion can be drawn about the longitudinal distribution of secondary protons.

4. Conclusion

In order to study the waste transmutation effectiveness, as well as to examine the radiation effects due to the intense field of secondary hadrons emitted in the spallation environment of a sub-critical Accelerator Driven System,

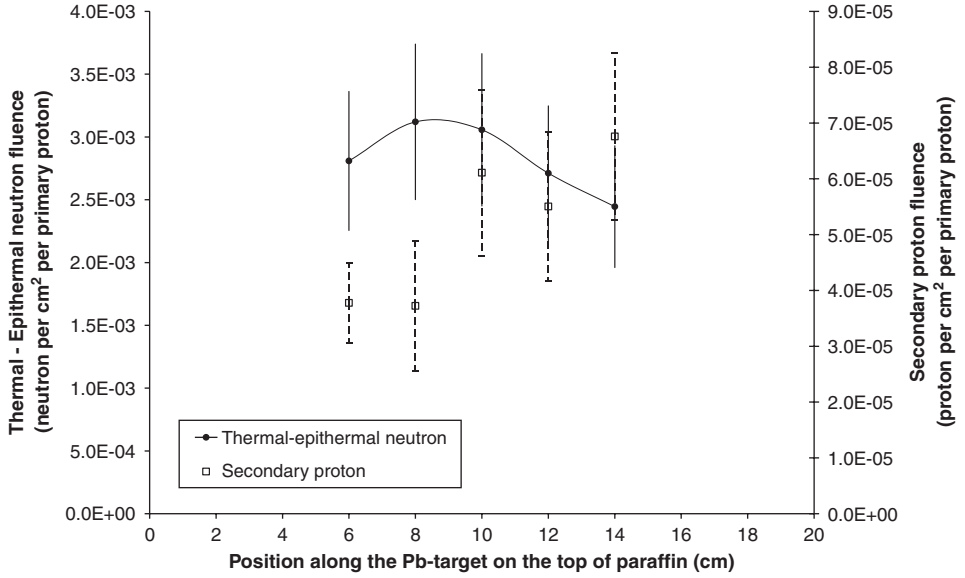

Fig. 7. Therma–epithermal neutron and secondary proton fluences along the Pb/Paraffin target irradiated by a proton beam of 1 GeV.

the secondary proton and neutron fluences have to be determined. ^{nat}Cd is shown to be a useful activation detector for this purpose as one can simultaneously determine the thermal–epithermal neutron fluence via the $^{nat}Cd(n,x)^{115}Cd$ reaction as also the secondary proton fluence via the $^{nat}Cd(p,x)^{111}In$ reaction.

Placing ^{nat}Cd foils as activation detectors along the cylindrical mantle of spallation Pb/Paraffin target irradiated with a 1 GeV proton beam it is found that the thermal–epithermal neutron fluence in the energy range up to 1 keV depending on the position is between one and two orders of magnitude higher than the secondary proton fluence in the energy range from 10 to 100 MeV. This result is in reasonable agreement with the result from model calculations using the DCM-DEM code. In addition, an accumulation of thermal–epithermal neutrons around the center of the target (i.e. after approx. 10 cm) and of secondary protons towards the end of the target is observed. To strengthen these conclusions, the ^{nat}Cd activation method should be applied to different targets and for various proton beam energies.

References

Adam, J., et al., 2002. Transmutation of ^{239}Pu and other nuclides using spallation neutrons produced by relativistic protons reacting with massive U-and Pb targets. Radiochim. Acta 90, 431–442.

Adloff, J.C., et al., 1999. Secondary neutron production from thick Pb target by light particle irradiation. Radiat. Meas. 31, 551–554.

Andriamonje, S., et al., 1995. Experimental determination of the energy generated in nuclear cascades by a high energy beam. Phys. Lett. B 348, 697–709.

Bauer, G.S., 2001. Physics and technology of spallation neutron sources. Nucl. Instrum. Methods A 463, 505–543.

Brandt, R., et al., 1999. Transmutation studies using SSNTD and Radiochemistry and the associate production of secondary neutron. Radiat. Meas. 31, 497–506.

Carminati, F., et al., 1993. An Energy Amplifier for Cleaner and Inexhaustible Nuclear Energy Production Driven by a Particle Beam Accelerator. CERN, Geneva (Print CERN/AT/93-47 (ET)).

Hashemi-Nezhad, S.R., et al., 1999. Studies on neutron production in the interaction of 7.4 GeV protons with extended lead target. Radiat. Meas. 31, 537–544.

Kovalenko, A.D., et al., 1994. Spallation neutron source with hard energy spectrum for detector component testing at the Dubna Synchrophasotron. JINR Rapid Commun 1 (64), 12–25.

Krivopustov, M.I., et al., 1997. First experiments on transmutation studies on I-129 and Np-237 using relativist protons of 3.7 GeV. J. Radioanal. Nucl. Chem. 222, 267–270.

Krivopustov, M.I., et al., 2003. First experiments with a large uranium blanket within the installation energy plus transmutation exposed to 1.5 GeV protons. Kerntechnik 68, 48–55.

Nortier, F.M., et al., 1990. Excitation functions and production rates of relevance to the production on ^{111}In by proton bombardment of ^{nat}Cd and ^{nat}In up to 100 MeV. Appl. Radiat. Isot. 41, 1201–1208.

Sosnin, A., 2003. Private communication.

Stoulos, S., et al., 2003. Application of activation methods on the Dubna experimental transmutation set-ups. Appl. Radiat. Isot. 58, 169–175.

TARC, Collaboration, 1999. Neutron-driven nuclear transmutation by adiabatic resonance crossing. Final Report to EC, EUR19117, ISBN 92-828-7759-0.

Tárkányi, F., et al., 1994. Cross section of proton induced nuclear reactions on enriched ^{111}Cd and ^{112}Cd for the production of ^{111}In for use in nuclear medicine. Appl. Radiat. Isot. 45, 239–249.

Wan, J.S., et al., 1998. Transmutation of radioactive waste with the help of relativistic heavy ions. Kerntechnik 63, 167–177.

Wan, J.S., et al., 2001. Transmutation of ^{129}I and ^{237}Np using spallation neutrons produced by 1.5, 3.7 and 7.4 GeV protons. Nucl. Instrum. Methods A 463, 634–652.

Zaitseva, N.G., et al., 1990. Excitation functions and yields for ^{111}In production using $^{113,114,nat}Cd(p,xn)^{111}In$ reactions with 65 MeV protons. Appl. Radiat. Isot. 41, 177–183.